

Modern Physics Letters A
 Vol. 28, No. 16 (2013) 1330011 (16 pages)
 © World Scientific Publishing Company
 DOI: 10.1142/S0217732313300115



THE LARGE HADRON ELECTRON COLLIDER

OLIVER BRÜNING

CERN, 1211 Geneva 23, Switzerland
oliver.bruning@cern.ch

MAX KLEIN*

Physics Department, University of Liverpool, Oxford Street, L69 7ZE Liverpool, UK
max.klein@cern.ch

Received 12 April 2013

Accepted 12 April 2013

Published 13 May 2013

An overview is given on key physics, detector and accelerator aspects of the LHeC including its further development with emphasis to its role as the cleanest microscope of parton dynamics and a precision Higgs facility.

Keywords: Deep inelastic scattering; strong coupling; gluon; Higgs particle; linac.

PACS Nos.: 12.38.-t, 14.70.Dj, 14.80.Bn, 29.20.Ej

1. Deep Inelastic Scattering

The scattering of leptons off protons has led to fundamental insight and corresponding historic progress in particle physics. In 1955, with a beam of $E_e = 0.2$ GeV electron energy, a finite proton radius of about 0.74 fm was discovered. Using a higher energy beam, of $E_e \simeq 10$ GeV, the measurement of the proton structure function $\nu W_2 = F_2(x, Q^2)$ at fixed Bjorken x as a function of the four-momentum transfer squared Q^2 , performed by the famous SLAC-MIT experiment, established the existence of partons as the smallest constituents of protons.¹ Ten years later, in 1978, a measurement of the polarization asymmetry in ep scattering at very low Q^2 determined the right-handed weak isospin charge of the electron to be zero,² which was crucial for the identification of the Glashow–Weinberg–Salam theory as the appropriate description of the electroweak interaction. The first electron–proton collider, HERA, was built at DESY in eight years between 1984 and 1992.

*Corresponding author

It extended the Q^2 range up to a few times 10^4 GeV² and explored the region of very low $x = \frac{Q^2}{sy} \geq 10^{-4}$, for $s = 4E_e E_p \simeq 10^5$ GeV² and the inelasticity $y \leq 1$. With HERA, deep inelastic scattering (DIS) physics made enormous progress in the understanding of the proton's structure, of the quark–gluon dynamics and its theoretical description within quantum chromodynamics (QCD) and also in the search for new phenomena beyond the Standard Model (SM) of particle physics.³ There would nowadays be no quantitative description of LHC physics and notably the Higgs production cross-section, which at the LHC is dominantly due to gluon–gluon (gg) fusion, would not be known without the parton dynamics information deduced mainly from HERA.

The Large Hadron electron Collider (LHeC) is the next logical and a big step in the evolution of DIS physics as part of the accelerator exploration of the energy frontier. New phenomena in DIS may appear at high masses of new particles, as the Higgs or leptoquarks, at very high Q^2 exceeding the masses squared of the weak bosons W and Z and also at very low $x \propto \frac{1}{s}$ which at the LHeC extends down to $x \simeq 10^{-6}$. The LHeC kinematic range exceeds HERA's by a factor of about 20, due to the combination of a 7 TeV proton beam from the LHC and a new 60 GeV electron beam. Its luminosity is projected to be as high as possibly 10^{34} cm⁻²s⁻¹, with a default design value of 10^{33} cm⁻²s⁻¹. This is almost a thousand times higher than HERA's luminosity, and it makes the LHeC a potential precision Higgs production facility and enables a huge variety of new measurements and searches.

There was unfortunately no time given to operate HERA with deuterons nor heavy ions. Therefore, the knowledge from lepton–nuclear scattering currently relies on fixed target data only. The LHeC extends the kinematic range with deep inelastic electron–ion scattering by almost four orders of magnitude. A huge discovery potential there appears in eA regarding new phenomena in nuclear parton dynamics, nuclear PDFs and the initial state of the quark–gluon plasma (QGP). At lower energies concepts for electron–ion colliders are also being developed.⁴

Basic LHeC design solutions have recently been laid out in detail in a refereed conceptual design report (CDR) on the physics, accelerator and detector concepts.⁵ These have been summarized in Ref. 6 and updated in Ref. 7 mainly in view of the Higgs discovery.^{8,9} The following paper presents the detector design concept, a few highlights of the physics program and summarizes the accelerator design as well as sketching directions for the future development of the LHeC.

2. LHeC Detector Design

The LHeC is the second electron–hadron collider following HERA. Its physics programme demands a very high level of precision, as for the measurement of the strong coupling constant α_s to per mille uncertainty, and it requires the reconstruction of complex final states, as appear in charged current Higgs production and decay into $b\bar{b}$ final states. As a consequence of the asymmetric electron and proton beam energy configuration, the detector acceptance has to extend as close as possible to the

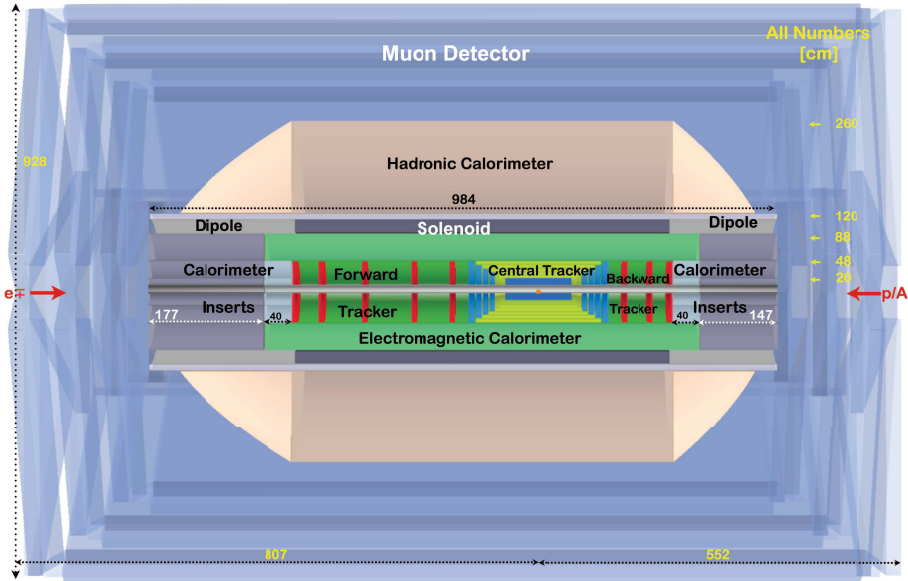


Fig. 1. (color online) An rz cross-section of the LHeC detector in its baseline design with the solenoid and dipole magnets placed between the electromagnetic and the hadronic calorimeters. The interaction point is surrounded by a central tracker system, complemented by large forward and backward tracker telescopes, and followed by sets of calorimeters, see text. The detector dimensions are ≈ 13.6 m longitudinally to the beam and ≈ 9.3 m in diameter, which may be compared with the CMS dimensions of 21×15 m².

beam axis. The dimensions of the detector are constrained by the radial extension of the beam pipe, elliptic due to synchrotron radiation, in combination with a polar angle coverage extending down to about 1° and 179° for forward going final state particles and backward scattered electrons at low Q^2 , respectively.

A cross-section of the central, baseline detector is given in Fig. 1. In the central barrel, the following detector components are currently considered: a central silicon pixel detector surrounded by silicon tracking detectors of strip or possibly strixel technology; an electromagnetic liquid argon (LAr) calorimeter inside a 3.5 T solenoid and a dipole magnet, with a 0.3 T field on axis, required to achieve head-on collisions; a hadronic tile calorimeter serving also for the solenoid flux return and a muon detector, so far for muon identification only, relying on the precise inner tracking for momentum measurements. The electron at low Q^2 is scattered into the backward silicon tracker and its energy is measured in backward calorimeters. In the forward region, components are placed for tracking and for calorimetry to precisely reconstruct jets over a wide energy range up to $O(\text{TeV})$.

Simulations of tracking and calorimeter performance were used to verify the design, while a full detector simulation is not yet available. The momentum resolution based on the central tracker is $\frac{\delta p_T}{p_T} = 6 \times 10^{-4} \text{ GeV}^{-1}$ which translates to a radial impact parameter resolution of $10 \mu\text{m}$. Combined with the extension of the beam

spot of $7 \mu\text{m}$ in both transverse directions this promises to be a very precise heavy quark tagging environment with the biggest challenge of a good forward direction performance. The simulated resolution of the central electromagnetic liquid argon calorimeter is $\frac{\sigma}{E} = \frac{8.5}{\sqrt{E/\text{GeV}}} \oplus 0.3\%$. The hadronic energy resolution, from a combined LAr and scintillator tile calorimeter simulation, with the magnets in between the calorimeters, is $\frac{\sigma}{E} = \frac{32}{\sqrt{E/\text{GeV}}} \oplus 8.6\%$.

The CDR⁵ also contains designs for forward and backward tagging devices for diffractive and neutron physics and for photo-production and luminosity measurements, respectively. The radiation level at the LHeC is much lower than in pp , and the ep cross-section is low enough for the experiment not to suffer from any pile-up, which are the two most demanding constraints for the ATLAS and CMS detectors and their upgrades for the HL-LHC. The choice of components for the LHeC detector can rely on the experience obtained at HERA, at the LHC, including its detector upgrades currently being developed, and also on detector development studies for the ILC. The detector development, while requiring prototyping, may therefore proceed without an extended R&D program.

The time schedule of the LHeC project is given by the LHC and its upgrade project, which demand a detector to be ready within about 10–12 years. A first installation study was made considering pre-mounting the detector at the surface, lowering and installing it at IP2. The detector is small enough to fit into the L3 magnet structure of 11.2 m diameter, which is still resident in IP2 and would be available as mechanical support. Based on the design, as detailed in the CDR, it is estimated that the whole installation can be done in 30 months, which appears to be compliant with the operations currently foreseen in the LS3 shutdown in the early '20s.

3. Physics with the LHeC

3.1. Overview

With its unprecedented precision, DIS range and resolution in probing partonic interactions, the LHeC has a huge scientific potential as has been elucidated in Ref. 5. By completely determining, for the first time, the proton, neutron and nuclear parton densities, it adds considerably to the capabilities of the existing LHC experiments and the HL-LHC upgrade program, for example in terms of precision studies of Higgs properties, see below, and sensitive range in high mass LHC searches, see Ref. 7. Following Ref. 6, one may classify the physics of the LHeC into six, partially overlapping research categories: (i) discoveries in QCD, Higgs, BSM and top quark physics; (ii) relations to the LHC; (iii) gluon distribution and precision DIS; (iv) parton structure of nucleons and photons, perturbative QCD and non-DGLAP evolution; (v) heavy-ion physics, including deuterons, and modified parton distributions (GPDs, diffractive, unintegrated) and (vi) extension of HERA measurements as of the longitudinal structure function or vector mesons produc-

tion. For the current overview, two most important and comprehensive subjects are selected here for a more detailed presentation, the precision measurement of α_s and the potential for Higgs physics with the LHeC, both being related to the determination of the gluon distribution.

Every step into a new region of phase space and intensity can lead to new observations as happened in DIS with the discoveries of scaling at SLAC or of the striking role of the gluon at HERA, the self-interaction of which gives mass to the baryonic matter. DIS with the LHeC may lead to discovering unexpected substructure phenomena, for example along speculations,¹⁰ of the heaviest known particles, the W , Z , top or even the Higgs to possess structure, or it may become crucial for disentangling contact interaction phenomena which could be observed at the LHC with multi-TeV mass scales. It may be discovered that there is *no* saturation of the gluon density, despite common belief, the odderon or instanton may eventually be found or, similarly, the application of PDFs to describe LHC phenomena could become questionable when factorization could be observed to not hold, not just in diffraction but possibly in inclusive scattering too. Nature keeps holding surprises which is the overriding reason for the LHeC to be built.

3.2. The strong coupling constant and precision DIS

DIS is an ideal process for the determination of the strong coupling constant, which determines the scaling violations of the parton distributions. Theory is presently calculated to NNLO in perturbative QCD with elements already available to N³LO, see Ref. 11. Despite major efforts over the past nearly 40 years, since the discovery of asymptotic freedom, and a plethora of α_s determinations, there is no accurate value of α_s available,¹² with a precision comparable to the weak coupling constant, and a number of severe problems remains to be solved. Questions regard the (in)consistency of previous DIS data, the (in)consistency of inclusive DIS and jet based determinations, both in DIS and Drell–Yan scattering, or the treatment leading to the world average on α_s and its uncertainty.¹³ The LHeC has the potential to provide a new, coherent data base, from neutral and charged current DIS including heavy quark parton distribution measurements, with which an order of magnitude improved experimental determination of α_s becomes possible. This is of crucial importance for QCD, for predictions of LHC cross-sections, notably that of the Higgs production, discussed below, and for the predictions of grand unification of the electromagnetic, weak and the strong interactions at the Planck scale. It is also long time to challenge the lattice QCD α_s results, which seem to be most accurate but stand on different grounds than the classic data based measurements exhibiting variations which are non-negligible.¹²

Two independent fit approaches have been undertaken in order to verify the potential of the LHeC to determine α_s . These analyses used a complete simulation of the experimental systematic errors of the NC and CC pseudo-data and higher-order QCD fit analysis techniques, see the CDR⁵ for details. The total experimental

uncertainty on α_s is estimated to be 0.2% from the LHeC alone and 0.1% when combined with HERA. Relying solely on inclusive DIS ep data at high Q^2 , this determination is free of higher twist, hadronic and nuclear corrections, unlike any of the recent global QCD fit analyses. There are known further, parametric, uncertainties in DIS determinations of α_s . These will be much reduced with the LHeC as it resolves the full set of parton distributions, $u_v, d_v, \bar{u}, \bar{d}, s, \bar{s}, c, b$ and xg for the first time, providing x and Q^2 dependent constraints not “just” through the fit procedure. The LHeC therefore has a huge power in the determination of PDFs which cannot be replaced nor challenged by the yet important constraints inherent in precision Drell–Yan data at the LHC.^a Recently a six-flavor variable number scheme has been proposed,¹⁴ in which it is predicted that the top contribution to proton structure has an on-set much below the threshold of its production in a massless scheme. This may lead to the concept of a top quark distribution which completed the set of PDFs measurable with the LHeC.

Regarding the challenging precision on α_s one needs to not only measure PDFs more accurately but control also the heavy quark theory and experimental input. The measurement of the charm structure function in NC at the LHeC will determine the charm mass parameter to 3 MeV, which is expected to correspond to an α_s uncertainty well below 0.1%. Due to the huge range in Q^2 and the high precision of the data, decisive tests will also become available for answering the question whether the strong coupling constants determined with jets and in inclusive DIS are the same. If confirmed, a joint inclusive and jet analysis has the potential to even further reduce the uncertainty of α_s .

Matching this outstanding experimental precision requires future LHeC based analyses on inclusive cross-sections to be performed at N³LO pQCD for reducing the scale uncertainty. The ambition to measure α_s to per mille accuracy thus represents a vision for a renaissance of the theoretical and experimental physics of DIS which is a major task and fascinating prospect of the LHeC enterprise.

3.3. Higgs in electron–proton scattering

In the SM, the Higgs field is responsible for generating masses of the weak gauge bosons as well as the elementary fermions, in a mechanism through absorption of Nambu–Goldstone bosons arising in spontaneous symmetry breaking. The simplest representation of the mechanism adds an extra field to the theory which is a scalar, $J^{CP} = 0^{++}$, that is referred to as the SM Higgs boson (H). Recent exciting developments following the discovery of a new boson of mass $M_H \simeq 125$ GeV by ATLAS⁸ and CMS⁹ indicate that this particle most likely indeed is the Higgs boson.

^aThis question is sometimes raised in discussions but it is clear that the determination of x and Q^2 in the DIS measurements, from both the scattered lepton and the hadron over a huge range of five orders of magnitude combined with the theoretical advantage of involving only one hadron is the appropriate way to measure PDFs. This becomes immediately obvious from the comparison of HERA and Tevatron results on PDFs, see also the discussion in Ref. 7.

The exploration of its properties has begun to become a focus of modern particle physics. The observed Higgs mass value leads to a rather large number of decay modes which will enable detailed investigations of the properties of that boson to be made. At the LHC, background, theoretical and experimental conditions, as large pile-up, make it not easy to achieve high precision Higgs related measurements. Therefore, various lepton–lepton and photon–photon collider configurations have been vigorously studied, while the genuine prospects of Higgs physics at the LHC are being investigated also, much related to ATLAS and CMS detector upgrade designs.

At the LHC, the Higgs is dominantly produced via a top loop in $gg \rightarrow H$ fusion. A smaller fraction stems from the associated WH or ZH production which lead to similar final states. The interest in Higgs physics with the LHeC primarily comes from its clean production mechanism, based on H emission from W or Z t -channel exchange in CC or NC scattering, and low QCD backgrounds. The cross-section of the SM Higgs production in polarized e^-p CC scattering^b is about 200 fb at the default LHeC energies of $E_e = 60$ GeV and $E_p = 7$ TeV. Therefore, the e^-p H production cross-section is about as large as the Z -Higgsstrahlung cross-section at an e^+e^- collider above $H + Z$ threshold energies. Compared to the LHC, the ep configuration has the advantage of a cleaner final state reconstruction due to the presence of only one hadronic vertex and the absence of pile-up. It is important also that the theoretical uncertainties of Higgs production in ep are small.¹⁵ The LHeC thus appears to be a very attractive facility for Higgs physics complementing the LHC and an e^+e^- machine.

Prior to the Higgs discovery, for the LHeC design a study was made of the prospect to reconstruct the decay of $H \rightarrow b\bar{b}$ as this dominates, to 60%, the branching fractions but is very difficult to precisely measure at the LHC for QCD background reasons. The result,^{5,7} from an initial cut based analysis, is a signal-to-background ratio of 1 and a statistics which allows to determine this cross-section to 3% statistical accuracy with 100 fb^{-1} of luminosity. This result has a number of implications: (i) it demonstrates that the ep collider has a huge potential for precision Higgs physics; (ii) with luminosities of order $10^{34} \text{ cm}^{-2}\text{s}^{-1}$ the LHeC will be of similar value as the ILC, and complementary access becomes possible to further decay modes such as into fermions $H \rightarrow \tau\tau, c\bar{c}$, both challenging at the LHC, c involving a second generation coupling, and also the H decay into bosons, $WW, ZZ, \gamma\gamma$, from a clean WW initial state, the former delivering a potentially clean measurement of the H to WW coupling; (iii) with the specific ep configuration unique measurements of the CP properties are in reach with access to CP odd admixtures and/or precision measurements of the CP even (SM) eigenvalues.¹⁸

^bThe cross-section in e^+p is lower, about 60 fb, due to the involvement of down instead of up quarks. Since very high luminosities in the linac-ring configuration will be limited to electrons and a high degree of polarization for positrons is unlikely achievable either, the e^+p configuration is inferior to e^-p for LHeC Higgs physics. In NC, the cross-section is about 20 fb.

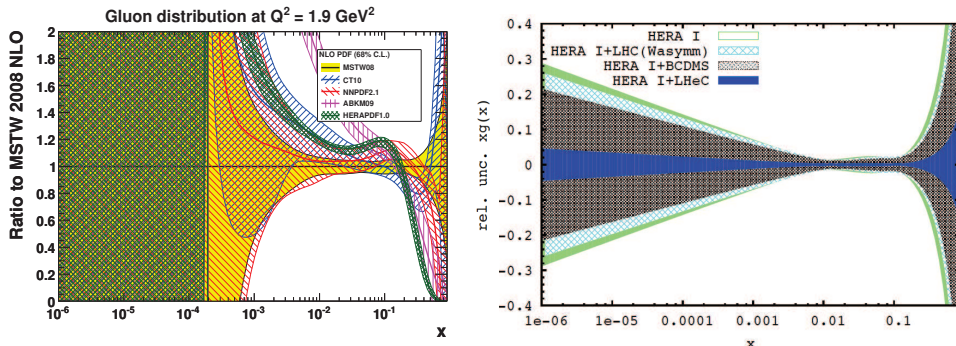


Fig. 2. (color online) Uncertainty of the gluon distribution at $Q^2 = 1.9 \text{ GeV}^2$ as a function of Bjorken x . Left: Recent gluon distribution determinations and their uncertainties, plotted as a ratio to MSTW08. Below $x \simeq 10^{-3}$ the HERA data have vanishing constraining power due to kinematic range limitations and the gluon is not determined at low x . It is for the LHeC to discover whether xg saturates or not and whether indeed the DGLAP equations need to be replaced by nonlinear parton evolution equations as BFKL.¹⁶ At large $x \geq 0.3$ the gluon distribution becomes very small and large variations appear in its determination, differing by orders of magnitude, which is related to uncertainties of jet data, theory uncertainties and the fact that HERA had not enough luminosity to cover the high x region where, moreover, the sensitivity to xg diminishes, as the valence quark evolution is insensitive to it. The situation can be expected to improve with LHC jet and possibly top¹⁷ and the HERA II data. Right: Experimental uncertainty of xg based on HERA alone and in various combinations, see the CDR.⁵ At large values of e.g., $x = 0.6$ the LHeC can be expected to determine xg to 5–10% precision (inner blue band). At small x a few percent precision becomes possible, compare right with left. Note that the non-LHeC low x uncertainty bands below $x \simeq 10^{-3}$ (right) are narrow solely as an artifact due to the parametrization of xg .

At the LHeC one probes new physics at the WWH and ZZH vertices with a simpler final state, no pile-up and knowing the directions of the struck quark. Measurements of couplings have to be precise as, for example, the H to WW and ZZ couplings, when measured with better than 8% accuracy, could allow accessing a composite Higgs structure.¹⁹ The prospects for Higgs physics with the LHeC are remarkable and deserve to be studied deeper.

A salient further aspect of ep assisting to make the LHC a precision Higgs physics facility is the superb measurement of the PDFs and α_s in ep with the LHeC. The dominant production mode for the Higgs in pp is gg fusion and therefore the cross-section is proportional to the product of α_s and xg squared. The LHeC leads to a much improved determination of the gluon density over five orders of magnitude in Bjorken x , extending to large x as illustrated in Fig. 2. This is at the origin of a huge improvement of the knowledge, based on pseudo LHeC data, of the Higgs production cross-section at the LHC, shown in Fig. 3 and calculated with $iHixs$,²⁰ in comparison with the available NNLO PDF determinations. It thus is possible to essentially remove or control the theory uncertainties of H measurements at the LHC which now are of the order of 10%, depending on PDF assumptions and the admixture of VH events in H data samples. Naturally this will lead to

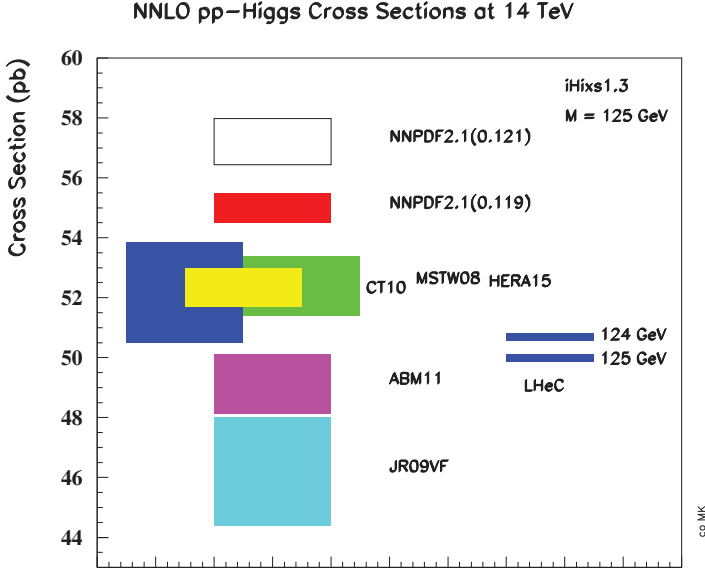


Fig. 3. (color online) NNLO calculation of the Higgs production cross-section in pp scattering at the design LHC energy using the *iHixs* program. The cross-section is calculated at a scale of $\frac{M_H}{2}$. The bands on the left side represent the uncertainties of the various PDF sets available to NNLO as marked. The PDF4LHC convention excludes ABM11, JR09VF, HERA and extreme values of α_s arriving in this calculation to roughly 5% uncertainty from PDF variations to which one would add an about 10% from scale uncertainty, as this picture looks different when M_H is used, see text, and about 5% due to α_s . The full experimental uncertainty estimated with the LHeC PDFs, as detailed in the CDR and plotted at the right column, is about 0.3%, with a similar uncertainty to be added from α_s discussed above. From these two sources therefore, the LHeC would provide the means to derive Higgs mass values from LHC cross-section measurements.

the requirement of N³LO cross-section calculations combined with most precise α_s and N³LO PDF determinations as can emerge in a decade hence with the LHeC and intense theoretical developments.^c The ILC in this context would provide a measurement of the width and precision data which delivered further insight even though the challenge to reach $10^{34} \text{ cm}^{-2}\text{s}^{-1}$ luminosities with positrons at the linear collider is considerable and the effort immense. Higgs physics can be done best with the combination of pp , ep and e^+e^- colliders. It may lead beyond the SM and the SM Higgs, which could be composite.²¹

^cThe scale dependence of the $gg \rightarrow H$ production cross-section at NNLO is still large. The choice of scales in pQCD calculations is to some extent arbitrary but indicative of missing higher-order terms. For $M_H = 125 \text{ GeV}$, at 14 TeV cms energy using *iHixs*, one obtains a cross-section of 52.5 pb with an uncertainty of (+1, -1.6)% for the MSTW08 PDF set using $\mu_r = \mu_f = \frac{M_H}{2} (\frac{1}{2}, \frac{1}{2})$, which gives the yellow band in Fig. 3. If instead one sets, as mostly is done, $\mu_r = \mu_f = M_H (1, 1)$, the cross-section is 47.9 pb, i.e. reduced by 9%. This is mainly due to the renormalization scale dependence as is seen by independent variations of μ_r and μ_f . The result is 53.1 pb and 47.2 pb for the cases $(\frac{1}{2}, 1)$ and $(1, \frac{1}{2})$, respectively.

4. Accelerator Design

4.1. LHeC project

The LHeC is an electron–proton (ep) and electron–ion (eA) complement of the Large Hadron (pp , pA and AA) Collider, with which lepton–quark interactions can be explored at the TeV energy scale. In summer 2012 an extensive report, the CDR, was published,⁵ in which a new electron beam accelerator was designed, as a ring mounted on top of the LHC (RR option) and as a multiple pass, energy recovery linac in a racetrack configuration (LR option), sketched in Fig. 4. The LHeC is designed to run simultaneously with pp (or AA) collisions. LHeC operation is fully transparent to the other LHC experiments thanks to the low lepton bunch charge and resulting small beam–beam tune shift experienced by the protons. After careful consideration of installation issues and parameters of the electron beam, preference was given to the LR option for the next phase of design as this is rather independent of the LHC. Early considerations of linac–ring electron–proton colliders were published in Refs. 22 and 23.

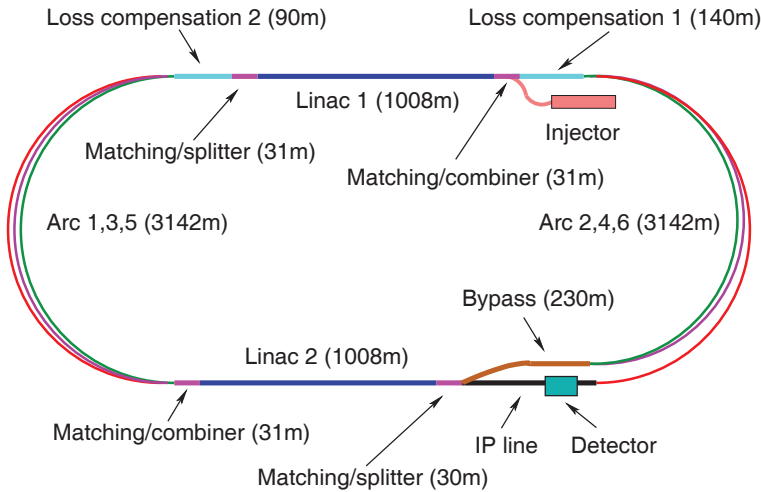


Fig. 4. (color online) Schematic view of the default LHeC racetrack configuration. Each linac accelerates the beam to 10 GeV, which leads to a 60 GeV electron energy at the interaction point after three passes through the opposite linear structures of 60 cavity–cryo modules each. The arc radius is about 1 km, mainly determined by the synchrotron radiation loss of the 60 GeV beam which is decelerated for recovering the beam power after having passed the IP. The default tunnel circumference is $\frac{1}{3}$ that of the LHC. The tunnel is designed to be tangential to IP2. Detailed civil engineering considerations are described in the CDR.

The LHeC design study has been pursued under the auspices of the European Committee for Future Accelerators (ECFA), the Nuclear Physics European Collaboration Committee (NuPECC) following a CERN SPC mandate. ECFA has released a supportive statement in November 2012, following the recommendations

of an ECFA study group, while NuPECC, already in 2010, decided to put the LHeC on the long range map for the future of European nuclear physics. The combination of high energy electron–proton and electron–ion physics makes the LHeC an important example which unites interests from accelerator based particle with nuclear physics. Following a mandate of CERN, a few years are now foreseen for next developing key LHeC technologies in international collaborations, see below.

4.2. Luminosity prospects and power consumption

The luminosity L for the LHeC in its linac-ring configuration is determined as

$$L = \frac{N_e N_p f \gamma_p}{4\pi \epsilon_p \beta^*}, \quad (1)$$

where $N_e = 10^9$ is the number of electrons per bunch, $N_p = 1.7 \times 10^{11}$ the number of protons per bunch, $f = \frac{1}{\Delta} = 40$ MHz the bunch frequency with the bunch distance $\Delta = 25$ ns, $\epsilon_p = 3.7 \mu\text{m}$ the normalized proton transverse beam emittance and $\beta^* = 0.1$ m the value of the proton beta function at the IP, assumed to be equal in x and y . The just quoted numbers are taken from the CDR. They correspond to the nominal LHC p beam parameters and lead to a peak luminosity of $10^{33} \text{ cm}^{-2}\text{s}^{-1}$. The electron beam current is given as

$$I_e = e N_e f = \frac{P}{E_e}, \quad (2)$$

where I_e is given in mA, P is the electron beam power, in MW, and E_e the electron beam energy in GeV. From the values above one derives that the current to reach $10^{33} \text{ cm}^{-2}\text{s}^{-1}$ under the quoted conditions is $I_e = 6.4$ mA. This corresponds to 384 MW beam power at $E_e = 60$ GeV. Given a 100 MW wall-plug power limit for the design this can only be realized in an energy recovery mode. This implies CW operation which can be realized with SC cavity gradients of about 20 MV/m for two linacs of 1 km length each. The configuration considered in the CDR uses $P_0 = 24$ MW linac grid power, which assumes an ERL efficiency of $\eta = 0.94$ and $P = \frac{P_0}{1-\eta}$. A total of 78 MW is foreseen assuming a cryogenics power consumption of 21 MW, which may be reduced with a quality factor Q_0 of the superconducting (SC) cavities exceeding the assumed 2.5×10^{10} , and 23 MW for the compensation of synchrotron losses in the return arcs. The quality of the SC cavity and mastering the ERL technique are critical to the success of the LHeC.

The luminosity may be further enhanced because the proton beam brightness, $\frac{N_p}{\epsilon_p}$, is expected to be larger by a factor of 2.5 than here assumed, the electron current may be doubled based on an enlarged Q_0 value and β^* could be reduced to 5 cm. If all these improvements were realized the LHeC would be an ep collider with a luminosity of $10^{34} \text{ cm}^{-2}\text{s}^{-1}$ enhancing substantially its Higgs and BSM physics potential. Small corrections to Eq. (1) are as discussed in the CDR, may be an hourglass reduction factor of 0.9, a luminosity enlargement for e^-p from pinch effects of 1.35, and perhaps a reduction to $\frac{2}{3}$ if a clearing gap was introduced for fast

Table 1. LHeC ep and eA collider parameters. The numbers give the default CDR values, with optimum values for maximum ep luminosity in parentheses and values for the ePb configuration separated by a comma.

Parameter [unit]	LHeC	
Species	e^-	$p, {}^{208}\text{Pb}^{82+}$
Beam energy (/nucleon) [GeV]	60	7000, 2760
Bunch spacing [ns]	25, 100	25, 100
Bunch intensity (nucleon) [10^{10}]	0.1 (0.2), 0.4	17 (22), 2.5
Beam current [mA]	6.4 (12.8)	860 (1110), 6
rms bunch length [mm]	0.6	75.5
Polarization [%]	90	none, none
Normalized rms emittance [μm]	50	3.75 (2.0), 1.5
Geometric rms emittance [nm]	0.43	0.50 (0.31)
IP beta function $\beta_{x,y}^*$ [m]	0.12 (0.032)	0.1 (0.05)
IP spot size [μm]	7.2 (3.7)	7.2 (3.7)
Synchrotron tune Q_s	—	1.9×10^{-3}
Hadron beam–beam parameter	0.0001 (0.0002)	
Lepton disruption parameter D	6 (30)	
Crossing angle	0 (detector-integrated dipole)	
Hourglass reduction factor H_{hg}	0.91 (0.67)	
Pinch enhancement factor H_D	1.35	
CM energy [TeV]	1300, 810	
Luminosity/nucleon [$10^{33} \text{ cm}^{-2}\text{s}^{-1}$]	1 (10), 0.2	

ion stability. Table 1 presents LHeC parameters, including, in parentheses, values for the increased luminosity version.

4.3. Components and frequency choice

In the CDR,⁵ designs of the magnets, RF, cryogenic and further components have been considered in quite some detail. Main parameters for both the RR and the LR configurations are summarized in Table 2. The total number of magnets (dipoles and quadrupoles excluding the few special IR magnets) and cavities is 4160 for the ring and 5978 for the linac case. The majority are the 3080 (3504) normal conducting dipole magnets of 5.4(4) m length for the ring (linac return arcs), for which short model prototypes have been successfully built, testing different magnet concepts at BINP Novosibirsk and at CERN as is described in the CDR. The number of high quality cavities for the two linacs is 960, possibly grouped in 120 cavity-cryo modules. This is an order of magnitude less than is required for the ILC. For the RF frequency values significantly below 1 GHz are suggested by beam dynamics studies,

Table 2. Selected components and parameters of electron ring (left) and linac (right) accelerators, taken from the LHeC CDR.

	Ring	Linac
Magnets		
Number of dipoles	3080	3504
Dipole field [T]	0.013–0.076	0.046–0.264
Number of quadrupoles	968	1514
RF and cryogenics		
Number of cavities	112	960
Gradient [MV/m]	11.9	20
Linac grid power [MW]	–	24
Synchrotron loss compensation [MW]	49	23
Cavity voltage [MV]	5	20.8
Cavity $\frac{R}{Q}$ [Ω]	114	285
Cavity Q_0	–	2.5×10^{10}
Cooling power [kW]	5.4@4.2 K	30@2 K

RF power considerations with NbTi grain and operating temperature effects and synchrotron loss compensation systems. The specific value has to be a multiple of the LHC bunch frequency and was recently chosen to be 802 MHz for genuine synergy with the HL-LHC higher harmonic RF system. The cryogenics system for the linac critically depends on the cooling power per cavity, which for the draft design is assumed to be 32 W at a temperature of 2 K. This leads to a cryogenics system with a total electric grid power of 21 MW. The development of a cavity-cryo module for the LHeC is directed to achieve a high Q_0 value and to reduce the dissipated heat per cavity, which will reduce the dimension of the cryogenics system.

4.4. Further accelerator developments

Following the publication of the CDR⁵ essential tests are now being prepared for various key components of the LHeC:

- Superconducting RF technology for the development of cavities with high Q_0 in CW operation;
- Superconducting magnet technology for the development of Nb₃Sn magnets for quadrupole designs with mirror cross-sections with apertures for high as well as low magnetic field configurations. This concerns specifically the prototyping of the Q_1 three-beam magnet nearest to the IP⁵;

- Optimization for the design of normal conducting magnets suited for the return arcs of the energy recovery options with multiple magnet systems (3 per arc);
- Design of an LHeC ERL Test Facility (LTF)²⁴ for studying and testing the various technical components and building up operational experience at CERN;
- Civil engineering studies for the linac-ring option including the connection of the electron and proton tunnels;
- Design of the vacuum and beam pipe system for the experimental insertion of the LHeC.

Further studies are foreseen of the full optics and layout integration of the LHeC into the high luminosity LHC project as well as a suitable design to maximize the positron intensity. The goal of these developments is to prepare the ground for deciding on the LHeC project later, in the context of the evolution of particle physics, in particular the LHC nominal beam energy results, and other projects at CERN and beyond. As a new opportunity to further exploit the LHC at CERN, the LHeC clearly requires strong international efforts.

4.5. *Time schedule and mode of operation*

The electron accelerator and new detector require a period of about a decade to be realized, based on experience from previous particle physics projects, as for example HERA, H1 and CMS. This duration fits with the industrialization and production schedules, mainly determined by the required ~ 3500 approximately 5 m long warm arc dipoles and the 960 cavities for the Linac. The current lifetime estimates and physics plans for the LHC are for two more decades of operation, which currently points to the shutdown LS3 for a major transition to this upgrade in the mid-'20s.

5. Summary

The LHeC is the natural, and the only possible successor of the DIS energy frontier exploration in the coming decades. It follows fixed target experiments at ~ 10 GeV and HERA at ~ 100 GeV of cms energy in order to study lepton-parton interactions at ~ 1000 GeV. Its physics program has key topics ($WW \rightarrow$ Higgs, RPV SUSY, α_s , gluon mapping, PDFs, saturation, eA) which all are closely linked to the LHC (Higgs, searches as for lepto-quarks and SUSY particles at high masses, QGP, etc.). With an electron beam upgrade of the LHC, the LHC can be transformed to a high precision energy frontier facility which is crucial for understanding new and "old" physics and possibly for the long term sustainability of the LHC program too.

The LHeC will deliver vital information for future QCD developments (N^3 LO, resummation, factorization, nonstandard partons, neutron and nuclear structure, AdS/CFT, non-pQCD, SUSY . . .). As a giant next step into DIS physics it promises to find new phenomena (gluon saturation, instantons, odderons, and speculatively substructure of heavy, so far elementary particles). A factor of almost 10^4 increase in kinematic range for electron-ion scattering leads to accessing the range of saturation

in the DIS region, where α_s is small, in both ep and eA , to shed light on the QGP and the mysteries of hadronization in media and outside.

The default electron beam configuration is a novel ERL (with less than 100 MW wall-plug power demand) in racetrack shape which is built toward the inside of the LHC ring and tangential to IP2. This is designed to deliver multi-100 fb⁻¹ of luminosity, i.e. more than a hundred times HERA's integrated luminosity. The LHeC is designed for synchronous operation with the LHC (three beams) and should be operational for the final decade of its lifetime. This gives 10–12 years for its realization. A detector concept is described in the CDR suitable for the linac-ring IR and to obtain full coverage and ultimate precision.

Half of the LHeC is operational. The other half requires next: an ERL test facility at CERN, IR related magnet and beam pipe prototype designs, to strengthen the LHC–LHeC physics links, to simulate and gradually to prepare for building the detector. The LHeC has a most attractive and important program worth to be pursued in order to maintain the diversity which collider particle physics needs to progress. It has also the potential to become a next Higgs factory.

Acknowledgments

This paper describes the effort of nearly 200 physicists in formulating the physics program, simulating major physics channels, designing a suitable detector system, and considering in much detail the accelerator options for a next and luminous electron–hadron collider. The authors are grateful to all their colleagues on LHeC and also to the CERN directorate for continuing encouragement and support in difficult times. We further wish to acknowledge the support of NuPECC and ECFA, the input from the about 20 project referees and especially the risen interest in making the vision of continuing DIS real.

References

1. E. D. Bloom *et al.*, *Phys. Rev. Lett.* **23**, 930; 935 (1969).
2. C. Y. Prescott *et al.*, *Phys. Lett. B* **77**, 347 (1978).
3. M. Klein and R. Yoshida, *Prog. Part. Nucl. Phys.* **61**, 343 (2008).
4. Ed. E. Metral, ICFA Beam Dynamics Newsletter, No. 58 (2012), <http://www-bd.fnal.gov/icfabd/Newsletter58.pdf>; EIC Study Group (A. Accardi *et al.*), arXiv:1212.1701.
5. LHeC Study Group (J. L. Abelleira Fernandez *et al.*), *J. Phys. G.* **39**, 075001 (2012).
6. LHeC Study Group (J. L. Abelleira Fernandez *et al.*), arXiv:1211.4831.
7. LHeC Study Group (J. L. Abelleira Fernandez *et al.*), arXiv:1211.5102.
8. ATLAS Collab. (G. Aad *et al.*), *Phys. Lett. B* **716**, 1 (2012).
9. CMS Collab. (S. Chatrchyan *et al.*), *Phys. Lett. B* **716**, 30 (2012).
10. C. Csaki, L. Randall and J. Terning, *Phys. Rev. D* **86**, 075009 (2012); A. De Simone, O. Matsedonskyi, R. Rattazzi and A. Wulzer, *JHEP* **1304**, 004 (2013).
11. J. Blümlein, *Prog. Part. Nucl. Phys.* **69**, 28 (2013).
12. S. Alekhin, J. Blümlein and S. Moch, *Phys. Rev. D* **86**, 054009 (2012).
13. S. Bethke *et al.*, arXiv:1110.0016.

14. C. Pascaud, Talk at DIS 2011, Newport News, USA, arXiv:1111.3262.
15. J. Blümlein, G. J. van Oldenborgh and R. Rückl, *Nucl. Phys. B* **395**, 35 (1993).
16. E. A. Kuraev, L. N. Lipatov and V. S. Fadin, *Sov. Phys. JETP* **45**, 199 (1977) [*Zh. Eksp. Teor. Fiz.* **72** (1977) 377]; I. I. Balitsky and L. N. Lipatov, *Sov. J. Nucl. Phys.* **28**, 822 (1978) [*Yad. Fiz.* **28**, 1597 (1978)].
17. M. Czakon, M. L. Mangano, A. Mitov and J. Rojo, arXiv:1303.7215.
18. S. S. Biswal, R. M. Godbole, B. Mellado and S. Raychaudhuri, *Phys. Rev. Lett.* **109**, 261801 (2012).
19. R. S. Gupta, H. Rzehak and J. D. Wells, *Phys. Rev. D* **86**, 095001 (2012).
20. C. Anastasiou, S. Buehler, F. Herzog and A. Lazopoulos, *JHEP* **1204**, 004 (2012).
21. D. B. Kaplan and H. Georgi, *Phys. Lett. B* **136**, 183 (1984).
22. P. Grosse-Wiesmann, *Nucl. Instrum. Meth. A* **274**, 21 (1989).
23. M. Tigner, B. Wiik and F. Willeke, *Proc. IEEE Particle Accelerator Conference*, San Francisco (1991), p. 2910.
24. R. Calaga, E. Ciapala and E. Jensen, CERN-LHeC-Note-2012-006 ACC (2013).